Available online at www.sciencedirect.com
ScienceDirect
Trans. Nonferrous Met. Soc. China 24(2014) 162−169
Transactions of Nonferrous Metals Society of China
www.tnmsc.cn

Compressive behavior of Zn−22Al closed-cell foams under uniaxial quasi-static loading

A. HEYDARI ASTARAIE, H. R. SHAHVERDI, S. H. ELAHI

Department of Materials Engineering, Tarbiat Modares University, P.O. Box 14115-143, Tehran, Iran

Received 31 December 2013; accepted 24 June 2014

Abstract: Zn−22Al alloy closed-cell foams were fabricated by melt foaming process using hydride foaming agent. The compressive properties were investigated under quasi-static condition. The structure of the foamed material was analyzed during compression test to reveal the relationship between morphology and compressive behavior. The results show that the stress−strain behavior is typical of closed-cell metal foams and mostly of brittle type. Governing deformation mechanism at plateau stage is identified to be brittle crushing. A substantial increase in compressive strength of Zn−22Al foams was obtained. The agreement between compressive properties and Gibson−Ashby model was also detected.

Key words: Zn−22Al foams; compression behavior; compressive strength; elastic modulus; modeling

1 Introduction

Closed-cell metal foams are defined as the solidified mixtures of gas bubbles and metallic liquids [1]. They are used as structural materials with a combination of unique properties, such as light-weight construction, energy absorption, sound absorption, vibration damping and thermal control [2]. Several methods have been used to manufacture closed-cell metal foams [3]. Among them, two methods, namely powder metallurgy and melt foaming, have mostly been utilized for foaming of metals [4]. Especially the melt foaming route, in which a foaming agent is added into molten metal, is relatively more suitable for commercial manufacturing of metal foams due to its low cost and ease of handle.

Although development of metal foams shows a relatively long-life history, the existing production techniques did not reach a satisfactory level as polymeric foams. BANHART [5] discussed the existing barriers to metal foam commercialization. He admitted that in order to overcome deficiencies, there remains a demand to explore the foaming behavior of potential materials other than aluminum alloys, which so far have been the main material for production of metallic foams, and to investigate the properties of resultant foams. In line with this, numerous researchers have developed non-aluminum foams, including iron [6], magnesium [7] and Zn-based foams. Regarding the available background and the recent research, it will be clear that Zn-based alloys, especially Zn−Al alloys, are one possibility owing to their inherent capabilities.

In the last decade, there have been several studies on the production and mechanical properties of foamed Zn−Al alloys. KOVACIK and SIMANCIK [8] processed Zn and ZnAl4Cu1 foams by powder metallurgy route with porosities ranging from 78% to 91% and reported that the compressive strength of foamed alloys is remarkably lower compared with aluminum foams with the same apparent density. However, they possess nearly the same compressive properties as aluminum foams at equal relative density. Zn−22Al closed-cell foams were fabricated by KITAZONO and TAKIGUCHI [9]. They found that the conventional powder metallurgy technique for Al foams can be successfully exploited for the production of Zn−22Al foams. They also pointed out that heat treated Zn−22Al foams demonstrate better energy absorption capacity in comparison with Alporas foam. LIU et al [10] manufactured Zn−22Al foams through melt foaming route using $CaCO_3$ blowing agent and investigated their compressive properties. YU et al [11] introduced SiC particles into molten Zn−22Al alloy and foamed the melt using carbonate foaming agent. LIU et al [12,13] repeated the same procedure for Al_2O_3 short

Corresponding author: H. R. SHAHVERDI; Tel: +98-21-82883307; Fax: +98-21-82883307E-mail: shahverdi@modares.ac.ir
DOI: 10.1016/S1003-6326(15)63591-9

fibers to enhance the compressive strength at relative densities higher than 0.16. Strain rate dependency of Zn−22Al foams was also studied with results showing remarkable strain rate sensitivity with strain rates ranging from 10^{-3} to 10^{3} s^{-1} [14] and up to 2×10^{-2} s^{-1} [9]. In addition, DAOUD [15] fabricated novel Zn12Al-based composite foams and investigated the compressive responses of foams at different strain rates. The results showed that the yield, plateau and plastic stress of composite foams were higher than those of Zn12Al foam.

It is evident that most of the researches have been focused on Zn−22Al alloy. Although there is not discussion much about this selection from Zn−Al alloys, it turns out to be a proper choice due to the combination of enhanced strength and reduced mass in final foamed material.

Metallic foams are cellular solids with a high level of porosity (typically with relative densities lower than 0.2). This is especially important when physical properties are intended to be used in final application in order to enhance the properties over counterparts [1]. This issue becomes even more significant when originally heavier metals like Zn-based alloys are incorporated. In fact, the total mass of foamed material is a secondary criterion for materials selection. Thus, to overcome the increased mass for Zn−22Al foams compared with Al foams, sufficiently low relative densities must be obtained. To the best of our knowledge, there are very few researches concerning this porosity range.

In this study, the compressive properties of Zn−22Al closed-cell foams with relative densities lower than 0.2 are investigated. It is shown that Zn−22Al foams could be produced with much higher mechanical properties. In addition, deformation mechanisms are discussed, which have not ever been identified for Zn−22Al foams.

2 Experimental

2.1 Production of Zn−22Al foams

Zn−22Al alloy with chemical composition of 22.30% Al, 0.47% Cu, and Zn balance was prepared. Calcium granules, 99% −9 mesh and zirconium hydride powder, 325 mesh, 99.7% (metal basis) were procured from Merck and Alfa Aesar Company, respectively. A stainless steel stirrer coated with alumina was used to produce foams.

Zn−22Al alloy pieces were melted in a graphite crucible in an electrical resistance furnace and 1% calcium was added to the melt. Then the melt was stirred for 10 min at the speed of 1200 r/min. The molten mixture was transferred into a preheated steel foaming mold coated with alumina. Zirconium hydride was added and dispersed through stirring at 1200 r/min for 30 s. The foaming mold was kept in the furnace without stirring at 500−550 °C to gain different relative densities. Then the mold was taken out and quenched in water in order to quickly solidify the liquid foam.

2.2 Compressive strength test

To investigate the mechanical properties of the produced foams, uniaxial compression tests were performed at room temperature. Cuboid specimens with dimensions of 35 mm×35 mm×45 mm were cut by electrical discharge machining (EDM). In order to eliminate the size effect known in metal foams [16], specimen dimensions were chosen such that the ratio of specimen size to cell size was ~10. Density of each specimen, ρ^*, was calculated from the measured mass and volume. Compression tests were conducted on an Instron model 5500R (6027). Load cell output was recorded with a personal computer. The direction of compression tests was the same as foaming direction. Specimen deformation was measured on the basis of crosshead movement of the plunger and strain was calculated using the initial specimen height. All the tests were done at the strain rate of 1×10^{-3} s^{-1}.

The first peak before load drop in the stress−strain curve was taken as the compressive strength, σ^*. The elastic modulus, E^*, was calculated from the slope of the unloading stress−strain curve by linear regression between stress levels of 1 MPa and $3/4\sigma^*$.

3 Results and discussion

3.1 Structure and morphology

Typical macroscopic view of the manufactured Zn−22Al alloy foam is shown in Fig. 1. The structure is typical of closed-cell metallic foams with a roughly equiaxed polyhedral cells (Fig. 1(a)) accompanied with imperfections which are frequently observed in metal foams. In addition to geometrical defects, fractured cell walls and very small pores in the cell nodes and cell edges are seen in the structure of the foams (Fig. 1(b)). Therefore, Zn−22Al alloy foam seems to be prone to many defects which may have considerable effects on the mechanical properties.

3.2 Compressive behavior

The stress−strain curves for produced Zn−22Al foams are seen in Fig. 2 as a function of the relative density. The observed stress−strain behavior resembles the one for other closed-cell metallic foams, which involves three distinct regions. At very early stage of loading, i.e. elastic region, stress changes linearly with strain. In the second stage called plateau region, the stress−strain curve is featured with a nearly constant

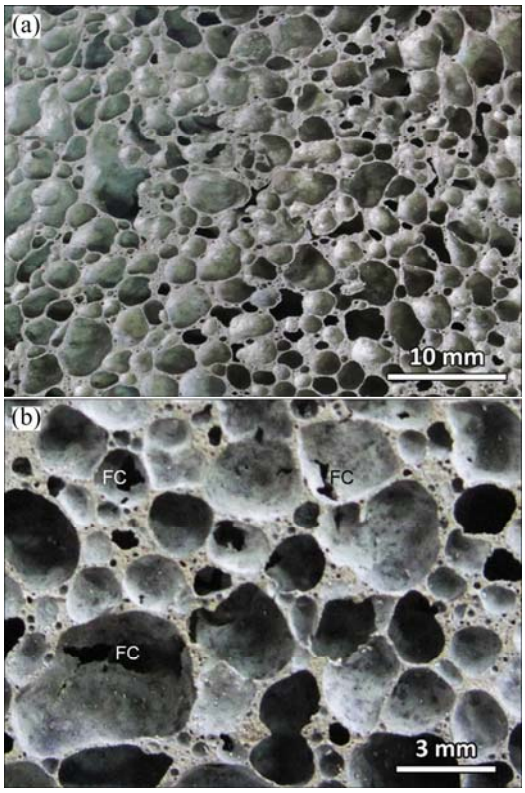

Fig. 1 Macrostructures of Zn−22Al foam (a) and detailed view of structure (b) (FC—fractured cell wall)

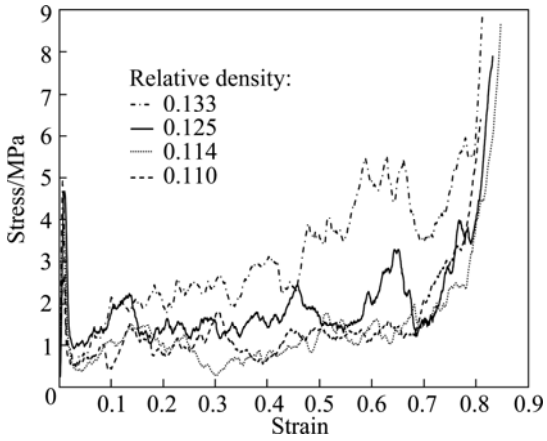

Fig. 2 Compressive stress−strain curves of Zn−22Al foams as function of relative density

stress in a wide range of strain. Finally, the stress grows rapidly with strain, forming the densification region in which cell walls contact each other.

A suitable approach to study the deformation mechanisms of metallic foams is to identify the collapse phenomena occurring at the plateau stage. The sequence of compression deformation for Zn−22Al foam with a relative density of 0.125 at elastic-plateau transition is shown in Figs. 3(a)−(c). The stress−strain curve for the

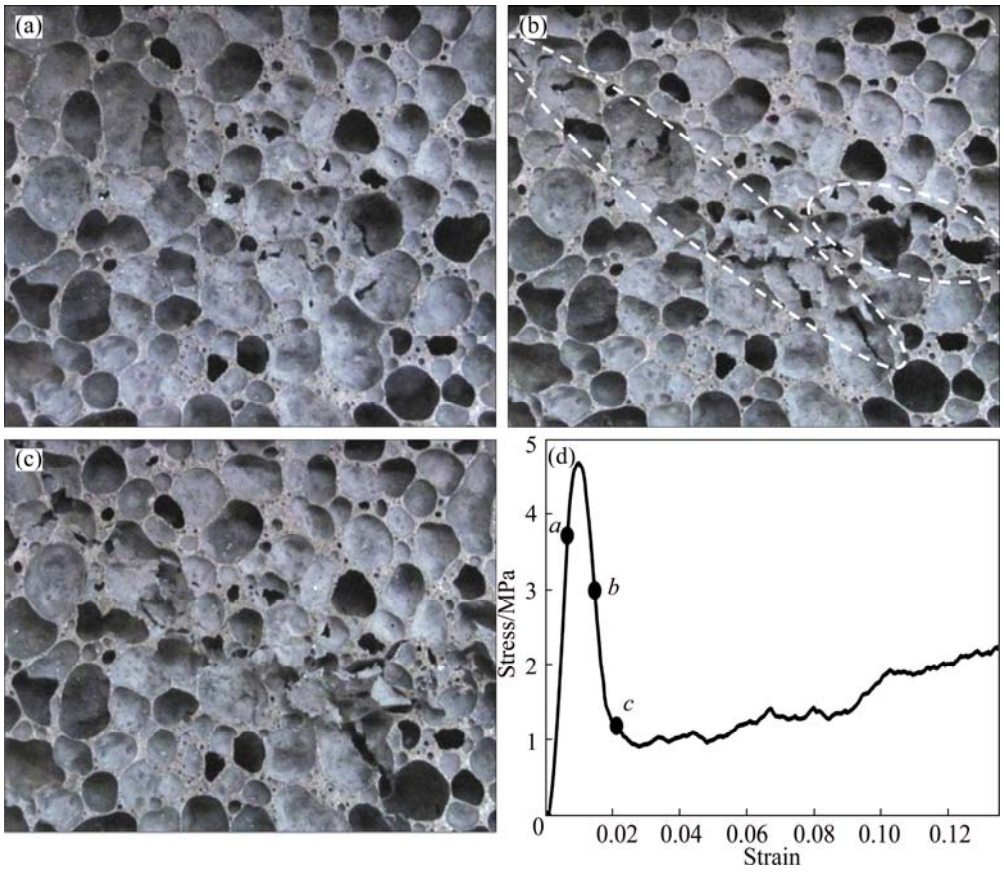

Fig. 3 Sequence of compression deformation for Zn−22Al alloy foam at elastic-plateau transition: (a)−(c) Cell structure during deformation; (d) Corresponding stress−strain curve

same foam has also been shown together with associated stages of deformation, labeled *a*, *b* and *c*, to trace the sequence (Fig. 3(d)). It is noted that the onset of plateau stage coincides with the occurrence of a peak in stress−strain curve and phenomena on unloading side of the peak will actually represent the collapse behavior.

Figure 3(a) shows the cell structure of the specimen before loading. As the loading goes on in elastic region, there reaches a peak after which the stress−strain curve starts to fall. As shown in Fig. 3(b), the onset of unloading is associated with occurrence of cracks normally close to an angle of 45°. These shear fractures most probably are connected with pre-cracks existing within the structure (Fig. 1(b)). The unloading proceeds down to point *c* in Fig. 3(d) where shear fractures connect to each other to make larger fractures (Fig. 3(c)).

Deformation mechanism of Al-based foams at plateau stage has been identified to be cell wall buckling for ductile Al-based foams [17], cell wall buckling/ tearing for Al-based brittle alloys [18] and Al−SiC composite foams with a lower content of SiC [19], and cell wall tearing for Al−SiC composite foams with a higher content of SiC [19]. In this regard, large shear fractures in Zn−22Al foams along with no evidence of buckling or bending of cell walls indicate that the main deformation mechanism is brittle crushing, which is the main collapse phenomenon at plateau stage. Brittle crushing is due to breaking of cell walls and cell edges during compression.

Deformation mechanisms of metallic foams have been divided into two distinct categories [17]: ductile and brittle. Ductile foams exhibit a smooth plateau in the stress−strain curve while brittle foams have a jagged and oscillatory plateau behavior. The stress−strain curves for Zn−22Al foams (Fig. 2) show many oscillations in their plateau region, proving a brittle nature of deformation. It has been identified that each oscillation is due to localization of deformation in a band and successive crushing of deformation bands leads to unsmoothed plateau appearance [17].

The brittle behavior of foams is a direct function of the brittleness of material existing in the structure of foam. Regarding the eutectoid microstructure of Zn−22Al alloys, the brittleness for these foams directly arises from brittle nature of as-cast Zn−22Al alloy with a very limited plasticity. As-cast Zn−Al alloys with high Al contents have a very poor ductility at ambient temperature, namely less than 3% of elongation [20]. The presence of non-metallic particles originating from Ca and blowing agent additions should also be taken into account which may add to brittleness. It should also be noted that in fully ductile Al foams, as discussed later, load drops are small, and introduction of intermetallics or ceramic particles into foamed aluminum adds simultaneously to brittleness and load drop [21,22]. Thus, larger load drops in Zn−22Al foams should accompany even a greater brittleness, which is consistent with essentially brittle behavior of Zn−22Al foams.

The load drop at the onset of plateau for Zn−22Al foams (Fig. 2) is relatively large compared with the one usually observed in Al foams. Load drops are small in Alporas type Al foams and get larger foams containing intermetallics [21] or ceramic particles [22]. But load drops for Zn−22Al foams (Fig. 2) are even larger and neither seem to be density dependent nor are recovered right after fall, namely, the load does not raise much after dropping. Such load drops are explainable concerning the formation of large shear fractures that extend throughout the specimen. In fact, because of the large shear fracture, the upper part of the foam makes a large move relatively to the lower part in the loading direction. The result is a tremendous reduction in stress or load.

THORNTON and MAGEE [23] have also reported similarly large load drops for pure zinc foams at relatively low temperatures. KOZA et al [24] have attributed the load drop in Al foams to the collapse of one cell layer, and the factor governing its extent has been stated to be the pore size. The larger the pore size, the greater the load drop. However, cell size distribution of Zn−22Al foams is mostly in the range of 2−4 mm (Fig. 1), and is also typical of most closed-cell metal foams. Thus, this factor plays only a minor role in stress drop of Zn−22Al foams.

3.3 Compressive strength

The compressive strength of closed-cell Zn−22Al foams is listed in Table 1 and is also plotted in Fig. 4 as a function of relative density. The curves are obtained by the best fit using the least squares method. It is seen that compressive strength of the foam increases with increasing relative density. As expected, there is a great dependency of compressive strength on the porosity. There also are data provided by LIU et al [10], which is the only available information on the compressive strength of as-cast Zn−22Al foams in the examined range of relative density. It is evident that the compressive

Table 1 Compressive properties of Zn−22Al foams in quasi-static loading

Specimen No.	Relative density	Compressive strength/MPa	Elastic modulus/GPa
1	0.092	2.73	0.85
2	0.110	3.21	1.143
3	0.114	3.85	1.226
4	0.125	4.68	1.35
5	0.133	4.94	1.612
6	0.149	6.01	1.97

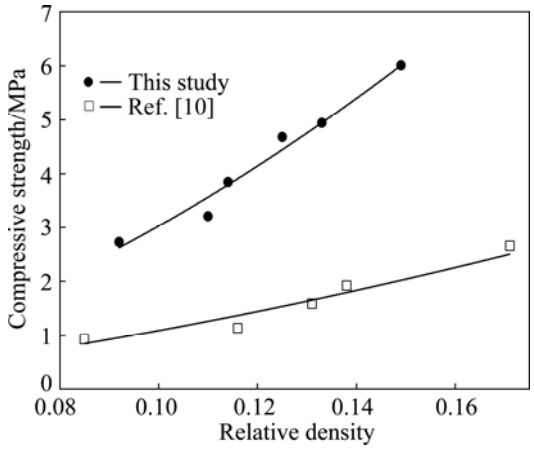

Fig. 4 Compressive strength of closed-cell Zn−22Al foams as function of relative density

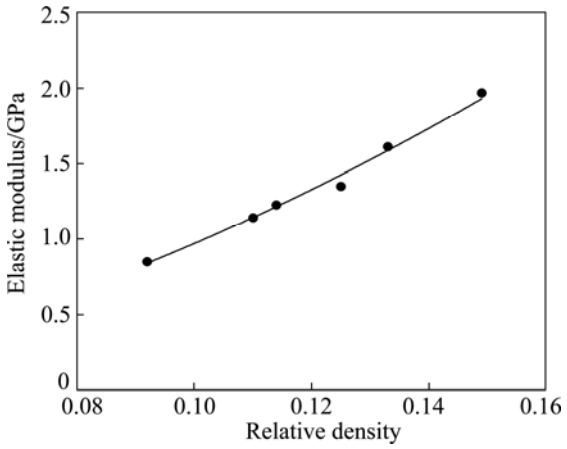

Fig. 5 Elastic modulus of closed-cell Zn−22Al foams as function of relative density

strength obtained in the current study is 170%−200% higher at a given relative density. It should be noted that chemical composition, strain rate and specimen dimensions are essentially same or even less conservative in the current study.

The observed discrepancy in compressive strength can be attributed to the morphology-related parameters (e.g., solid fraction in the cell walls, defects, cell size, etc.) and/or the difference in cell wall material strength. A considerable enhancing in morphology may occur as a result of employment of ZrH_2 blowing agent compared with $CaCO_3$. The applicability of $CaCO_3$ for the production of Zn−22Al foams becomes restricted regarding the great mismatch between temperature range for melting of Zn−22Al alloy and efficient gas release of blowing agent. Cell wall material strengthening might be another reason due to a lower foaming temperature and quenching the mold in water rather than cooling in air.

3.4 Elastic modulus

One of the most important properties of structural materials is the elastic behavior. Table 1 lists the elastic moduli for Zn−22Al foams, which is also plotted against relative density in Fig. 5. The curve is obtained by the best fit using the least squares method. It is observed that the elastic modulus increases with increasing relative density. It is also clear that the elastic modulus of Zn−22Al foams is a strong function of relative density. The elastic modulus is about 1 GPa at a relative density of 0.1 and increases to around 2 GPa at a relative density of 0.15. To the best of our knowledge, there are no data available in the literature on the elastic modulus of Zn−22Al foams.

3.5 Modeling

Modeling of the mechanical properties of metallic foams has drawn a great attention to itself, since it provides a simple way to estimate properties. The theoretical Gibson−Ashby model for the compressive strength of elastic−plastic closed-cell foams is given by [17]

$$\frac{\sigma^*}{\sigma_{ys}} = 0.3\left(\phi\frac{\rho^*}{\rho_s}\right)^{3/2} + (1-\phi)\left(\frac{\rho^*}{\rho_s}\right) \quad (1)$$

where ϕ is the solid fraction in the cell edges; ρ^* is the density of the foam; ρ_s is the density of the cell wall material; σ^* is the compressive strength of the foam; and σ_{ys} is the yield strength of cell wall material.

In addition, the model for the compressive strength of brittle closed-cell foams based on Gibson−Ashby methodology is

$$\frac{\sigma^*}{\sigma_{fs}} = 0.2\left(\phi\frac{\rho^*}{\rho_s}\right)^{3/2} + (1-\phi)\left(\frac{\rho^*}{\rho_s}\right) \quad (2)$$

which differs from Eq. (1) in the coefficient of the first term, and the yield stress is replaced by the modulus of rupture of cell wall material, notated by σ_{fs}.

Equation (2) consists of two terms, in which the first term considers the behavior of cell edges and the second term considers the behavior of cell walls [17]. It suggests that the deformation mechanism relates to the contribution from both cell edges and cell walls. In the case of an open-cell foam, where ϕ =1, there is no material in the cell walls, and Eq. (2) is reduced to

$$\frac{\sigma^*}{\sigma_{fs}} = 0.2\left(\frac{\rho^*}{\rho_s}\right)^{3/2} \quad (3)$$

As discussed earlier, the main deformation mechanism of Zn−22Al foams is brittle crushing rather than cell wall buckling. Thus, in the case of modeling the compressive strength of Zn−22Al foams, Eq. (2) (rather than Eq. (1) must be utilized. This is very important

since an incorrect choice of model will lead to incorrect predictions of collapse stress. In order to fit the strength data with Eq. (2), we need to know the modulus of rupture for the cell wall material. The modulus of rupture for many brittle materials is close to the fracture strength in uniaxial tension [17]. Therefore, fracture strength of Zn−22Al alloy, taken to be approximately 400 MPa [25], is used as a reasonable approximation for the modulus of rupture.

Figure 6 shows relative compressive strength of Zn−22Al foams together with Eq. (2) at ϕ values of 0.95 and 1.0. There is an inherent uncertainty in relative collapse stresses due to estimated value for the modulus of rupture. It is well-known that mechanical properties of as-cast Zn−Al alloys are a function of microstructure, and such factors as cooling rate, composition, porosity and inclusions are considered to be effective on it [26]. Considering ±50 MPa uncertainty interval for modulus of rupture, the interval for relative collapse stress is also displayed by error bars in Fig. 6. Nevertheless, it is obvious that the compressive strength falls close to and above the curve for ϕ=1.0 which corresponds to an open-cell foam model (equation (3)). It is noted that the curve for ϕ value of 0.95 is just an indicator to locate an upper bound for data and has no other special significance.

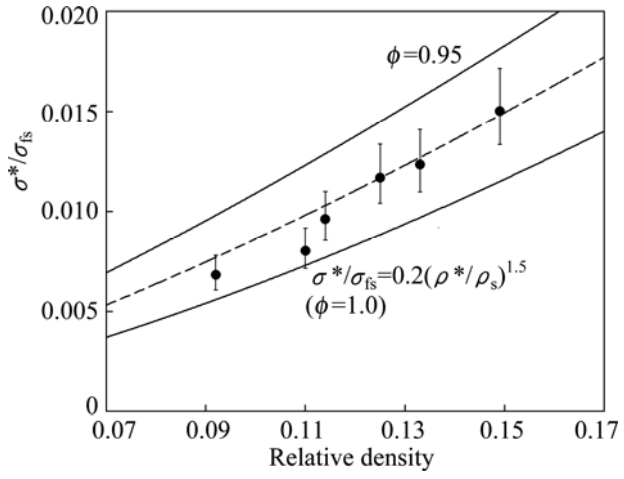

Fig. 6 Relative compressive strength against relative density together with Eq. (2) at ϕ values of 0.95 and 1.0

In the same way as compressive stress, the elastic modulus of closed-cell foams is modeled on the basis of cell edge and cell wall deformation which is given by

$$\frac{E^*}{E_s}=\phi^2\left(\frac{\rho^*}{\rho_s}\right)^2+(1-\phi)\left(\frac{\rho^*}{\rho_s}\right) \quad (4)$$

where E^* and E_s are the elastic modulus of the foam and cell wall material, respectively. For the case of open-cell foam (ϕ=1), Eq. (4) is reduced to the following relation:

$$\frac{E^*}{E_s}=\left(\frac{\rho^*}{\rho_s}\right)^2 \quad (5)$$

The normalized elastic modulus of Zn−22Al foams is plotted as a function of relative density in Fig. 7. The modulus for the cell wall material is taken to be 78 GPa for normalizing. The model curve for ϕ=1.0 is also included in Fig. 7, which corresponds to the case of open-cell foams. It is seen that elastic modulus data for Zn−22Al foams are settled closely and slightly higher than the model line for open-cell.

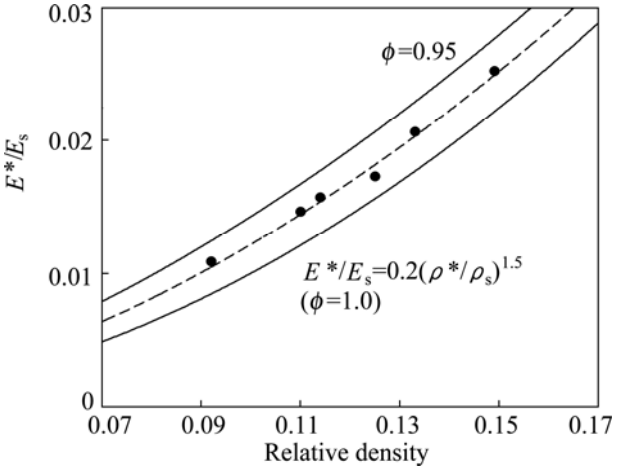

Fig. 7 Relative elastic modulus against relative density together with Eq. (4) at ϕ values of 0.95 and 1.0

Appearance of experimental data close to the model line for open-cell foams in Figs. 6 and 7 was anticipated because this behavior is well-known in Al-based metal foams [27]. This is also predictable noticing common ϕ values frequently observed in high porosity metal foams. GUDEN and YÜKSEL [19] tried calculating the value of ϕ for their foams using the relation proposed in Ref. [28] and showed a relatively good conformance with experimental results. The same procedure was applied to the current study to estimate ϕ value for produced Zn−22Al foams considering at least 20 cell edges. Regarding foams with different relative densities, ϕ values were measured to be in the range of 0.925−0.979, with the averaged value of 0.951.

An indirect method to calculate ϕ is the least squares fit of Gibson−Ashby relation with experimental data [21]. To accomplish this, experimental data for relative elastic modulus rather than relative collapse stress were used, since there is little or no uncertainty in estimating elastic modulus of cell wall material, and data presented in Fig. 7 can be regarded as accurate results. The best fit is shown in Fig. 7 by the dashed line. A value of 0.975 was identified for ϕ. There is a small difference

between measured (0.951) and fitted (0.975) values of ϕ. It is noted that the procedure used to calculate ϕ gives just an estimate, since this value is changing point by point within a foam structure, and averaging might not lead to the fitted value even considering a large number of cell edges. Model line for ϕ=0.975 is also plotted in Fig. 6 (dash line). It is observed that experimental data for relative collapse stress are described fairly well with the model line related to the ϕ value of 0.975.

4 Conclusions

This work focused on the compressive properties of Zn−22Al closed-cell foams fabricated by melt foaming. Occurrence of large shear fractures as well as sharp oscillations at plateau stage during compressive loading indicated that brittle crushing is the main deformation mechanism. A considerable enhancing in compressive strength was obtained compared with previous studies which may be due to the morphological and/or material-related improvements. It was found that the elastic modulus of Zn−22Al closed-cell foams increases with increasing relative density. Results show that the compressive strength and elastic modulus of Zn−22Al foams fit appropriately the Gibson−Ashby model for brittle closed-cell foams.

References

[1] BANHART J. Manufacture, characterization and application of cellular metals and metal foams [J]. Prog Mater Sci, 2001, 46: 559−632.

[2] BANHART J. Metal foams — From fundamental research to applications [C]//Frontiers in the Design of Materials (FDM 2005). Chennai, India: Universities Press (India) Limited, 2005: 279−289.

[3] KÖRNER C, SINGER R F. Processing of metal foams—Challenges and opportunities [J]. Adv Eng Mater, 2000, 2(4): 159−165.

[4] LEFEBVRE L P, BANHART J, DUNAND D C. Porous metals and metallic foams: Current status and recent developments [J]. Adv Eng Mater, 2008, 10: 775−787.

[5] BANHART J. Metal foams: Production and stability [J]. Adv Eng Mater, 2006, 8: 781−794.

[6] SMITH B H, SZYNISZEWSKI S, HAJJAR J F, SCHAFER B W, ARWADE S R. Steel foam for structures: A review of applications, manufacturing and material properties [J]. J Constr Steel Res, 2012, 71: 1−10.

[7] NEU T R, MUKHERJEE M, GARCIA-MORENO F, BANHART J. Magnesium and magnesium alloy foams [C]//Porous Metals and Metallic Foams. Seoul: GS Intervision, 2012: 139−146.

[8] KOVACIK J, SIMANCIK F. Comparison of zinc and aluminium foam behaviour [J]. Kovove Mater, 2004, 42: 79−90.

[9] KITAZONO K, TAKIGUCHI Y. Strain rate sensitivity and energy absorption of Zn−22Al foams [J]. Scr Mater, 2006, 55: 501−504.

[10] LIU J, YU S, ZHU X, WEI M, LUO Y, LIU Y. The compressive properties of closed-cell Zn−22Al foams [J]. Mater Lett, 2008, 62: 683−685.

[11] YU S, LIU J, LUO Y, LIU Y. Compressive behavior and damping property of ZA22/SiCp composite foams [J]. Mater Sci Eng A, 2007, 457: 325−328.

[12] LIU J A, YU S R, HU Z Q, LIU Y H, ZHU X Y. Deformation and energy absorption characteristic of Al_2O_{3f}/Zn−Al composite foams during compression [J]. J Alloys Compd, 2010, 506: 620−625.

[13] LIU J, YU S, ZHU X, WEI M, LI S, LUO Y, LIU Y. Effect of Al_2O_3 short fiber on the compressive properties of Zn−22Al foams [J]. Mater Lett, 2008, 62: 3636−3638.

[14] LIU J, YU S, SONG Y, ZHU X, WEI M, LUO Y, LIU Y. Dynamic compressive strength of Zn−22Al foams [J]. J Alloys Compd, 2009, 476: 466−469.

[15] DAOUD A. Effect of strain rate on compressive properties of novel Zn12Al based composite foams containing hybrid pores [J]. Mater Sci Eng A, 2009, 525: 7−17.

[16] ANDREWS E W, GIOUX G, ONCK P, GIBSON L J. Size effects in ductile cellular solids. Part II: Experimental results [J]. Int J Mech Sci, 2001, 43: 701−713.

[17] GIBSON L J, ASHBY M F. Cellular solids, structure and properties [M]. 2nd ed. Cambridge, UK: Cambridge University Press, 1997.

[18] LEHMHUS D, BANHART J. Properties of heat-treated aluminium foams [J]. Mater Sci Eng A, 2003, 349: 98−110.

[19] GUDEN M, YÜKSEL S. SiC-particulate aluminum composite foams produced from powder compacts: Foaming and compression behavior [J]. Mater Sci, 2006, 41: 4075−4084.

[20] ASM Metal's Handbook [M]//Properties and Selection of Nonferrous Alloys and Special-purpose Materials. US: ASM International, 2000.

[21] RAJ R E, DANIEL B S S. Structural and compressive property correlation of closed-cell aluminum foam [J]. J Alloys Compd, 2009, 467: 550−556.

[22] SUGIMURA Y, MEYER J, HE M Y, BART-SMITH H, GRENSTEDT J, EVANS A G. On the mechanical performance of closed cell Al alloy foams [J]. Acta Mater, 1997, 45: 5245−5259.

[23] THORNTON P, MAGEE C. Deformation characteristics of zinc foam [J]. Metall Mater Trans A, 1975, 6: 1801−1807.

[24] KOZA E, LEONOWICZ M, WOJCIECHOWSKI S, SIMANCIK F. Compressive strength of aluminium foams [J]. Mater Lett, 2003, 58: 132−135.

[25] ABOU EL-KHAIR M T, DAOUD A, ISMAIL A. Effect of different Al contents on the microstructure, tensile and wear properties of Zn-based alloy [J]. Mater Lett, 2004, 58: 1754−1760.

[26] BARNHURST R J, GEREVAIS E. Gravity casting of zinc–aluminum alloy: Dependence on soundness, microstructure, and inclusion content [J]. AFS Trans, 1983, 93: 591−602.

[27] ANDREWS E, SANDERS W, GIBSON L J. Compressive and tensile behaviour of aluminum foams [J]. Mater Sci Eng A, 1999, 270: 113−124.

[28] SIMONE A E, GIBSON L J. Effects of solid distribution on the stiffness and strength of metallic foams [J]. Acta Mater, 1998, 46: 2139−2150.

闭孔泡沫 Zn−22Al 在单轴准静态加载下的压缩行为

A. HEYDARI ASTARAIE, H. R. SHAHVERDI, S. H. ELAHI

Department of Materials Engineering, Tarbiat Modares University, P.O. Box 14115-143, Tehran, Iran

摘　要：通过使用氢化物发泡剂，采用熔体发泡法制备闭孔泡沫 Zn−Al 合金，在准静态条件下研究其压缩性能。在压缩试样过程中，分析发泡材料的结构，并研究其形态和压缩性能之间的关系。结果表明，应力−应变行为具有典型的闭孔泡沫金属和脆性泡沫金属的特征；在平稳阶段的控制变形机制是脆性破碎；泡沫 Zn−22Al 合金的抗压强度得到了显著提高，其压缩性能符合 Gibson−Ashby 模型

关键词：泡沫 Zn−22Al；压缩行为；抗压强度；弹性模量；建模

(Edited by Xiang-qun LI)